

Article

Spatial and Seasonal Variations of Standardized Photosynthetic Parameters under Different Environmental Conditions for Young Planted *Larix olgensis* Henry Trees

Qiang Liu and Fengri Li *

Department of Forest Management, School of Forestry, Northeast Forestry University, Harbin 150040, China; qiangliu2015@126.com

* Correspondence: fengrili@nefu.edu.cn; Tel.: +86-451-8219-0609

Received: 4 July 2018; Accepted: 27 August 2018; Published: 29 August 2018



Abstract: Understanding the spatial and seasonal variations in leaf physiology is critical for accurately modeling the carbon uptake, physiological processes and growth of entire canopies and stands. For a 17-year-old *Larix olgensis* Henry plantation, vertical whorl-by-whorl sampling and analyses of seasonally repeated measurements of major photosynthetic parameters were conducted, and the correlations between photosynthetic parameters and environmental conditions, leaf morphological traits and spatial position within the crown were analyzed. According to the correlations, the photosynthetic parameters were standardized based on the environmental conditions to avoid the influence of the changing environment on the patterns of spatial and seasonal variations of photosynthetic parameters. The results showed that the standardized light-saturated net photosynthetic rate (SP_{max}), standardized dark respiration (SR_d) and standardized stomatal conductance under saturated light (Sg_{s-sat}) were all negatively related to the relative depth into the crown (RDINC) throughout the growing season. However, their vertical patterns were different during the development of the phenological phase. In addition, different gradients of environmental conditions also influenced the values and the range of the vertical variation in photosynthesis. High temperature and low humidity usually resulted in smaller values and weaker vertical variations of SP_{max} and Sg_{s-sat} , but larger values and more obvious vertical variations in SR_d . SP_{max} and Sg_{s-sat} usually exhibited a parabolic seasonal pattern in different vertical positions within the crown; however, SR_d generally followed a concave pattern. These seasonal patterns were all weaker with increasing RDINC. Different environments also exhibited a significant influence on the seasonal patterns of photosynthesis. We suggested that standardization is necessary before analyzing spatial and seasonal variations. A single environmental condition could not represent the spatial and seasonal patterns under all gradients of the environment. Spatial and seasonal variations should be simultaneously analyzed because they are related to each other.

Keywords: environmental conditions; light-saturated net photosynthetic rate; dark respiration; stomatal conductance; relative depth into crown; leaf mass per area; leaf temperature; vapor pressure deficit; *Larix olgensis* Henry

1. Introduction

Light-saturated net photosynthetic rate (P_{max}), dark respiration (R_d) and stomatal conductance (g_s) are representative photosynthetic parameters that generally exhibit significant spatial variations, especially in the vertical direction [1–4]. Detailed information about the vertical variations of photosynthesis largely affects the accuracy of carbon uptake estimations, which promotes the evolution

of eco-physiological models from big-leaf models to multilayer models [5]. Multilayer estimations of carbon uptake contribute to the determination of the functional crown range of a tree crown or canopy [6,7], which can provide guidance in artificial pruning and, consequently, improve the economic value of timber [8,9]. For short trees, P_{\max} and R_d generally decrease with increasing depth into the crown [1,4,10] because the light environment is the core factor determining leaf development [10–14]. This behavior is more obvious in dense stands. However, it has been suggested that the dominant mechanism restricting leaf photosynthesis is water potential or hydraulic constraints, which increase with tree height [2,15–19], and this phenomenon is more obvious in tall tree species [17–19]. To adapt to vertical variations of environmental conditions, leaves usually express a significant vertical variation of morphological characteristics. Leaf mass per area (LMA) is one of the most important morphological characteristics [20–24]. The vertical LMA patterns are the result of the adaptation of leaves to both the light environment [11,14,20] and hydraulic constraints [25]. Moreover, LMA is closely associated with mesophyll conductivity to carbon dioxide [3,26] and consequently usually exhibits strong correlations with photosynthetic indicators [24,27,28].

The vertical patterns of leaf photosynthesis markedly change with phenological phases [19]. During the growing period, leaf functional traits vary as a result of the dynamic performance of leaf ontogeny and the environmental conditions [19,29]. For example, P_{\max} generally demonstrates a parabolic seasonal pattern, which is widely attributed to the phenological phase changes in mean leaf temperature, solar irradiance and soil moisture [30–33]. LMA usually increases rapidly during the leaf-expanding phase [32,34,35], which is caused by the accumulation of secondary metabolites [16,27,34,36] and is followed by the flattening or declining of the varied climatic conditions, e.g., light conditions [31,37] or soil water content [35,38,39]. In addition, other factors that have been suggested to affect photosynthesis to a certain extent include leaf age [10,15,33], distance to branch base [16] and sex [32,40], but these factors are more applicable to evergreen tree species and dioecious tree species.

The spatial and seasonal variations of leaf photosynthetic traits play important roles in the attempt to understand the constraints on carbon uptake [19,34,41–43] and in models of physiological processes [44,45] and the growth [46–49] of entire canopies and stands. Incorrect simulations occur when modeling the long-term carbon uptake if the spatial and seasonal variations in photosynthesis [19,29,41–43] or morphology [35,50] are neglected.

Most previous investigations on the spatial variations of photosynthesis-related leaf traits indicated that environmental conditions such as leaf temperature (T_{leaf}) and vapor pressure deficit (VPD) were always controlled within a similar range during measurements [3,11,27,50–52], which was usually a result of slight weather variations during the measurement process. However, environmental effects should be considered when studying the seasonal patterns of photosynthesis because seasonal fluctuations of the environment can be pronounced [34,39,53]. However, other studies have declared that environmental conditions could also maintain relatively stable values [33,54], or these studies have simply eliminated the “outliers” that markedly deviated from the average levels [34] or even directly overlooked the impacts of environmental changes [26,32,38,55,56].

T_{leaf} can be controlled with a photosynthetic apparatus but is limited by the difference between the ambient temperature and target temperature (acceptable range is ± 5 °C), while VPD is almost impossible to control during measurements, especially when measuring light or CO₂ response curves. It is unclear how the effects of environmental conditions should be treated when analyzing the vertical and seasonal patterns of photosynthesis, particularly in areas with sharply fluctuating environmental conditions. Moreover, it is unclear whether the spatial and seasonal patterns under a certain environmental condition could represent the effects of all gradients of environmental conditions, even if the environment can be controlled.

Larix olgensis Henry is an apparently light-demanding, cold-resistant but shade-intolerant tree species that has the advantages of fast growth, strong adaptability and high economic value [57,58]. *Larix olgensis* is one of the main afforestation tree species and accounts for 36% of the planted

area and 37% of the planted volume in northeastern China. *Larix olgensis* has been identified as a major fast-growing and high-yielding tree species in northeastern China [59]. Research on the photosynthetic characteristics of larch has been reported [60–67], but only a few studies have examined the photosynthetic characteristics of *Larix olgensis* [65–67]. Most previous studies have focused on diurnal changes or the response of photosynthetic characteristics to different concentrations of nitrogen or phosphorus rather than their spatial and seasonal variations. Liu et al. [65] analyzed spatial differences in crown photosynthesis in *Larix olgensis* but did not explain the reason for these spatial differences. Wang et al. [62] proved that the seasonal changes in the photosynthetic capacity of *Larix kaempferi* Sarg. depend on chlorophyll content. Galvagno et al. [63] and Kurachi et al. [64] proved that air temperature was the main factor influencing the seasonal variations of photosynthesis. However, they did not consider the comprehensive influence of all possible factors.

In this study, we hypothesize that the photosynthetic indicators mainly depend on the environmental conditions, needle morphology and vertical position within the crown. The objectives of this study are (i) to analyze the correlations between T_{leaf} , VPD, LMA and relative depth into crown (RDINC) and P_{max} , R_d and $g_{\text{s-sat}}$ (light-saturated stomatal conductance); (ii) to standardize P_{max} , R_d and $g_{\text{s-sat}}$ depending on the above correlations; and (iii) to analyze the spatial and seasonal patterns of standardized photosynthetic parameters under different gradients of environmental conditions.

2. Materials and Methods

2.1. Site Description

The experiments were conducted in 2017 at the experimental forest farm of Northeast Forestry University in Maoershan, which is 80 km southeast of Harbin, China (45°23'21" N, 127°37'56" E; altitude: 370 m above sea level). The site is characterized by a midlatitude monsoon climate, with warm, wet summers and cold, dry winters. The growing season for deciduous tree species is approximately five months, i.e., from early May (the end of the frost period) to the middle of September (the first frost). The average temperature throughout the growing season at the site is 17.0 °C (with a range from −1.3 °C to 39.4 °C), the average precipitation through the growing season is 944 mm, and the majority of the precipitation in the study period fell from June to August. The type of soil is typic Eutroboralfs [68], and the total forest coverage is approximately 83.3%, including 14.7% plantation.

2.2. Sample Selection

In this study, five sample plots (20 m × 30 m) were established within 17-year-old pure *Larix olgensis* plantations of the same habitat. The diameter at breast height (DBH) and tree height (H) were measured for each tree whose DBH was greater than 5 cm in each plot, and the quadratic mean diameters (Dg) for five plots were calculated independently. Then, five sample trees with DBH values respectively similar to the Dg of the five plots were selected to represent the average state of each plot. The attributes of the sampling plots and corresponding sampled trees are listed in Table 1. Scaffoldings were built around each sample tree to ensure that measurements could be performed at every crown position. The crown depths of the sample trees were divided into several vertical segments based on the pseudowhorls [69] from top to bottom within the crown. Previous work was conducted to analyze the horizontal differences in the photosynthetic light response (PLR) curves of the branches before the photosynthetic needle samples were selected (unpublished data), and the results showed that the PLR curves of the needles from the middle of a foliated branch adequately represented the average PLR curves of the entire branch (Figure 1a). Thus, three healthy and fully expanded needle clusters located within each segment in the middle of the foliated branches in sunny, semisunny and shaded crowns were selected (Figure 1b only presents the needle samples in sunny crowns and shaded crowns).

Table 1. Attributes of sample plots and corresponding sample trees for *Larix olgensis* Henry plantation.

Sample Trees				Sample Plots				
Tree NO.	DBH (cm)	H (m)	Plot NO.	Range of DBH (cm)	Range of H (m)	Quadratic Mean Diameter (cm)	Mean H (m)	Stand Density (trees ha ⁻¹)
I	10.75	10.33	P1	5.0–16.0	6.0–12.8	9.92	9.23	2200
II	11.15	10.52	P2	5.3–15.9	5.3–13.2	10.59	10.19	2400
III	10.90	10.81	P3	5.2–14.1	7.1–10.5	9.73	9.62	3200
IV	10.80	10.35	P4	5.0–16.7	5.8–13.0	10.13	9.63	2920
V	11.69	10.80	P5	5.2–16.5	6.3–12.7	10.92	10.3	2430

Note: Tree NO. = tree number, DBH = diameter at breast height, H = tree height; Plot NO. = plot number.

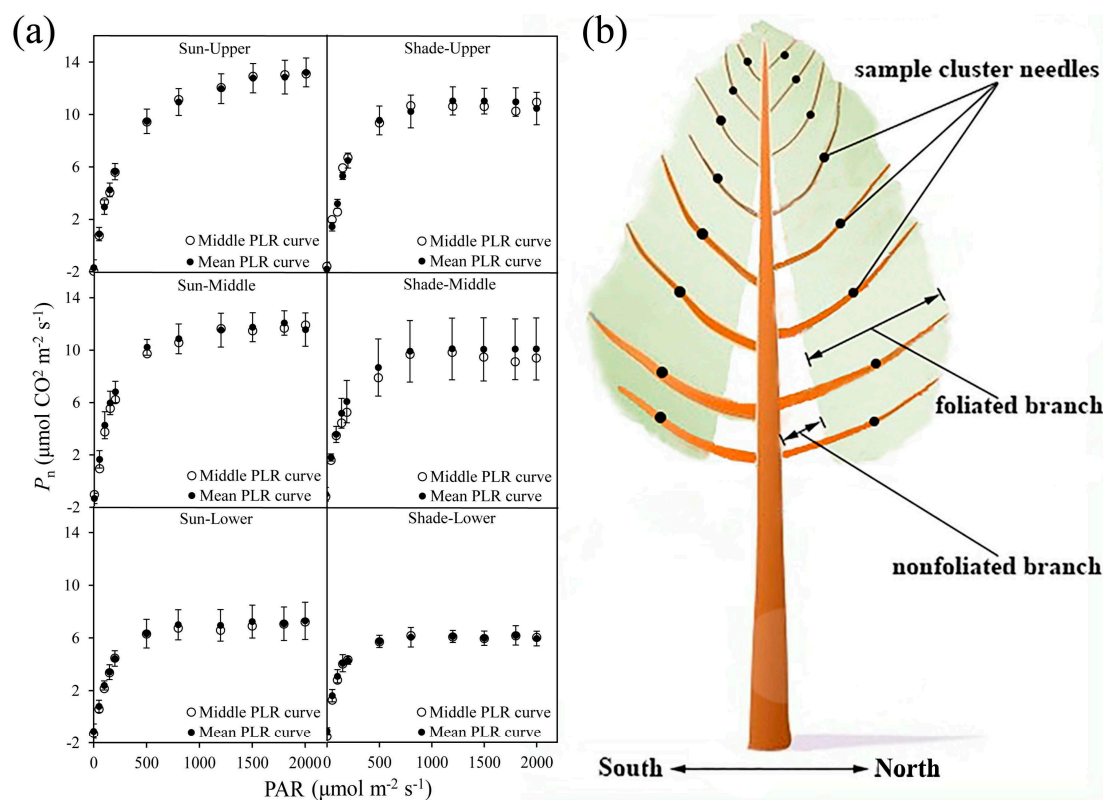


Figure 1. Positions of needle cluster samples within the crown. (a) Comparison between the PLR curve in the middle of the foliated branch and the average PLR curve throughout the entire foliated branch. P_n and PAR represent the net photosynthetic rate ($\mu\text{mol m}^{-2} \text{s}^{-1}$) and the photosynthetically active radiation ($\mu\text{mol m}^{-2} \text{s}^{-1}$), respectively; unfilled circles represent the PLR curve in the middle of the foliated branch, and filled circles represent the mean values of all PLR curves of the branch; and solid bars represent the standard deviation. (b) A diagram of the positions of needle cluster samples within the crown. PLR, photosynthetic light response; PAR, photosynthetically active radiation; P_n , net photosynthetic rate.

2.3. Photosynthetic Gas Exchange Measurements

Photosynthetic gas exchange measurements were conducted every half-month during the 2017 growing season in eight measurement campaigns (P, from 1 to 8): 15–25 May (P1), 1–10 June (P2), 15–25 June (P3), 1–10 July (P4), 15–25 July (P5), 1–10 August (P6), 15–25 August (P7) and 1–10 September (P8). All photosynthetic properties were measured using a portable steady-state photosynthesis system (LI-6400XT, LI-COR, Inc., Lincoln, NE, USA) equipped with a standard LED light source (6400-02B, LI-COR, Inc., Lincoln, NE, USA). The system was calibrated at the beginning and end of the season. The needle cluster samples were acclimated for 20 min at a CO_2 concentration

of 370 ppm, which is close to the actual CO₂ concentration within the crown. A CO₂ mixer (6400-01, LI-COR, Inc., Lincoln, NE, USA) was used to maintain a stable CO₂ supply in the chamber, and a PAR (photosynthetically active radiation) of 1400 $\mu\text{mol m}^{-2} \text{s}^{-1}$ was used to induce the needles for at least 10 min. This value was preliminarily confirmed to ensure saturating light conditions for all needle cluster samples (Figure 1a). PLR curves were measured at 17 PAR intensities in the following order: 2200; 2000; 1800; 1600; 1400; 1200; 1000; 800; 600; 400; 200; 150; 100; 60; 40; 15; and 0 $\mu\text{mol m}^{-2} \text{s}^{-1}$. The needle cluster samples were allowed to equilibrate for a minimum of 2 min at each step before the data were logged. The RDINC of each needle cluster sample was recorded when measuring the PLR curves. All measurements were conducted under ambient conditions with no control except for the CO₂ concentration in the chamber (stabilized at 370 ppm). The environmental variables (i.e., air temperature, T_{air} and VPD) outside the chamber were measured using a dynamic weather station (DL16, Adolf Thies GmbH & Co., KG, Göttingen, Germany) at 30-min intervals.

2.4. Photosynthetically Active Radiation Measurements

The crowns of the sample trees were equally divided into four directions horizontally based on the azimuth: eastern (45–135°), southern (135–225°), western (225–315°) and northern (<45° and >315°). In each vertical segment within the crown, PAR values evenly distributed in each direction were measured. The measurements were conducted from 8:00 a.m. to 16:00 p.m. at 2-h intervals on a clear day by using the LI-190s (LI-COR, Inc., Lincoln, NE, USA) quantum sensor, which was mounted on the sensor head of a portable steady-state photosynthesis system (LI-6400XT). We hypothesized that the vertical distribution of PAR within the crown would not significantly vary after the needle fully expanded, and thus the measurements of PAR were conducted only once, in August.

2.5. Leaf Morphology Measurements

Once the photosynthetic gas exchange measurements were completed, the photosynthetic needle cluster samples were taken immediately to measure the LMA (g m^{-2}). All samples were scanned immediately after collection and then surveyed with an image editor (Image-Pro Plus 6.0, Media Cybernetics, Bethesda, MD, USA) in the laboratory, resulting in a projected leaf area. The corresponding needles were then directly dried at 105 °C to a constant weight and weighed. The LMA was calculated by dividing needle dry mass by the corresponding projected leaf area.

2.6. Photosynthetic Parameters

The P_{max} ($\mu\text{mol m}^{-2} \text{s}^{-1}$) and R_d ($\mu\text{mol m}^{-2} \text{s}^{-1}$) were estimated from the PLR curves using the modified Mitscherlich model [70].

$$P_n = P_{\text{max}} \times \left(1 - e^{(-\alpha \times \text{PAR} / P_{\text{max}})}\right) - R_d \quad (1)$$

where P_n is the net photosynthetic rate ($\mu\text{mol m}^{-2} \text{s}^{-1}$), P_{max} is the light-saturated net photosynthetic rate ($\mu\text{mol m}^{-2} \text{s}^{-1}$), α is the apparent quantum yield, PAR is the photosynthetically active radiation ($\mu\text{mol m}^{-2} \text{s}^{-1}$), and R_d is the dark respiration rate ($\mu\text{mol m}^{-2} \text{s}^{-1}$).

The light-saturated g_s ($g_{s\text{-sat}}$) was determined as the corresponding g_s value of P_{max} . The statistics of the sample trees and branches are listed in Table 2.

Table 2. Descriptive statistics of the photosynthetic parameters, leaf morphology and corresponding environmental conditions.

RDINC	Statistics	Photosynthetic Parameters			Leaf Morphology	Environmental Conditions		
		P_{\max} ($\mu\text{mol m}^{-2} \text{s}^{-1}$)	R_d ($\mu\text{mol m}^{-2} \text{s}^{-1}$)	$g_{s\text{-sat}}$ ($\text{mol m}^{-2} \text{s}^{-1}$)	LMA (g m^{-2})	T_{leaf} ($^{\circ}\text{C}$)	VPD (kPa)	PAR ($\mu\text{mol m}^{-2} \text{s}^{-1}$)
0.1–0.2	Sample number	$n = 1299$ (99 PLR curves)						$n = 104$
	Mean	14.67	1.48	0.25	83.61	29.62	1.74	913.85
	Std	4.9	0.6	0.13	19.47	3.33	0.66	427.96
	Max	28.77	2.93	0.61	127.53	38.15	4.05	1879.79
	Min	5.57	0.58	0.05	29.18	19.53	0.78	58.04
0.2–0.3	Sample number	$n = 1026$ (80 PLR curves)						$n = 348$
	Mean	11.47	1.5	0.17	74.44	30.32	2.06	836.3
	Std	3.33	0.59	0.09	15.42	2.92	0.82	472.67
	Max	18.41	2.85	0.51	108.67	39.37	4.32	1998.87
	Min	5.23	0.31	0.04	31.07	25.07	0.97	104.9
0.3–0.4	Sample number	$n = 953$ (73 PLR curves)						$n = 1406$
	Mean	10.96	1.17	0.16	65.44	28.43	1.79	663.86
	Std	3.31	0.5	0.08	14.63	3.19	0.73	517.09
	Max	17.79	2.51	0.41	90.94	35.58	3.55	2006.43
	Min	4.7	0.18	0.04	26.64	19.74	0.83	14.27
0.4–0.5	Sample number	$n = 912$ (69 PLR curves)						$n = 1910$
	Mean	9.9	1.03	0.14	60.4	28.53	1.77	550.91
	Std	2.53	0.52	0.07	13.99	3.42	0.79	496.74
	Max	15.02	2.15	0.3	84.9	36.07	3.64	1804.97
	Min	3.21	0.31	0.02	24.85	20.42	0.65	7.86
0.5–0.6	Sample number	$n = 835$ (62 PLR curves)						$n = 2076$
	Mean	8.78	0.96	0.12	56.01	27.83	1.84	444.87
	Std	2.17	0.46	0.06	12.39	3.51	0.72	465.05
	Max	13.24	2.29	0.29	75.77	34.54	3.55	1856.4
	Min	4.41	0.19	0.03	28.85	19.71	0.67	7.45
0.6–0.7	Sample number	$n = 802$ (61 PLR curves)						$n = 2793$
	Mean	7.57	0.8	0.11	49.96	27.19	1.7	276.86
	Std	1.82	0.34	0.05	9.96	3.42	0.6	348.78
	Max	13.69	1.65	0.28	69.83	34.2	3.76	1781.77
	Min	4.33	0.3	0.03	29.3	18.96	0.81	6.44
0.7–0.8	Sample number	$n = 884$ (66 PLR curves)						$n = 2841$
	Mean	6.79	0.75	0.1	45.17	26.91	1.66	198.29
	Std	1.91	0.36	0.04	8.73	3.42	0.55	305.57
	Max	14.87	1.91	0.24	64.23	34.2	3.33	1609.52
	Min	3.17	0.25	0.03	26.22	18.5	0.75	2.79
0.8–0.9	Sample number	$n = 816$ (63 PLR curves)						$n = 2572$
	Mean	6.55	0.85	0.1	40.6	26.85	1.62	119.02
	Std	1.81	0.46	0.05	7.04	3.93	0.51	230.04
	Max	11.92	2.13	0.23	54.49	33.46	3.01	1463.72
	Min	3.47	0.2	0.03	26.86	15.45	0.64	1.54
0.9–1.0	Sample number	$n = 907$ (67 PLR curves)						$n = 2282$
	Mean	5.55	0.66	0.09	37.53	26.79	1.59	76.58
	Std	1.71	0.4	0.04	7	3.63	0.52	180.25
	Max	10.99	1.84	0.24	58.73	34.38	3.07	1477.64
	Min	2.1	0.17	0.03	23.98	17.8	0.64	1.04

Note: RDINC is the relative depth into the crown, P_{\max} is the light-saturated net photosynthetic rate, R_d is the dark respiration rate, $g_{s\text{-sat}}$ is the light-saturated stomatal conductance, LMA is the leaf mass per area, T_{leaf} is the leaf temperature, VPD is the vapor pressure deficit, n is the sample number, Std is the standard deviation, Max is the maximum value, Min is the minimum value. There are no data in the range of RDINC from 0 to 0.1 because this range corresponds to the tip of the tree, and there are no branches in this segment.

2.7. Statistical Analysis

As the environmental conditions, except for CO_2 concentrations (stabilized at 370 ppm), were not maintained at a certain value during the PLR curve measurements, the correlations between the photosynthetic parameters and environmental conditions (T_{leaf} and VPD) were analyzed using correlation analysis. In addition, the relationships between the photosynthetic parameters and leaf morphology (LMA) and vertical position within the crown (RDINC) were analyzed. Then, the regression equations between the photosynthetic parameters and the combinations of T_{leaf} , VPD, LMA and RDINC were established based on their relationships. Afterward, the photosynthetic parameters were standardized to any given environmental condition according to the regression equations to avoid the influence of pronounced fluctuations of environmental conditions during the whole phenological phase. The coefficient of determination (R^2) and root mean square error (RMSE)

were used to evaluate the performance of the regression equations. All statistical analyses were carried out using SAS 9.3 (SAS Institute Inc., Cary, NC, USA).

3. Results

3.1. Environmental Conditions

The main climate type of the study area is midlatitude monsoon with a volatile seasonal pattern (Figure 2). T_{air} and VPD demonstrated similar changes and were higher in July and August but lower in the other months of the growing season. The diurnal maximum/mean T_{air} and maximum/mean VPD changes were abrupt during the seasonal transitions. The maximum values of daily T_{air} and VPD reached 39.3 °C (Figure 2a) and 4.77 kPa (Figure 2c), respectively, at midday and appeared on the same day (5th July), while the minimum daily maximum T_{air} and VPD were 3.5 °C and 0.75 kPa (both on 6th May), respectively. The daily RH (relative humidity) and soil moisture (volumetric water content (VWC), %) also frequently and evidently varied during the study period. The daily mean RH was obviously higher than the daily minimum RH (Figure 2b), but there was not a marked difference between the daily mean VWC and minimum VWC (Figure 2d). Although the growing season showed a relatively high daily mean RH value, dry conditions still appeared at the beginning of August. The sharply diurnal fluctuations of weather make it almost impossible to maintain stable environmental conditions during the measurements of photosynthesis, especially among different seasons. Thus, it is necessary to eliminate the influence of changing environments before analyzing the spatial and seasonal variations in the photosynthetic parameters.

3.2. Relationships between Photosynthetic Parameters Versus T_{leaf} , VPD, LMA and RDINC

T_{leaf} and VPD represent the main environmental factors, and LMA and RDINC represent the main morphological characteristic and vertical position within the crown of leaves, respectively. The relationships between the photosynthetic parameters and the above factors are exhibited in Figure 3. P_{max} was significantly related to T_{leaf} and VPD (Figure 3a,b), in which P_{max} was positively correlated with T_{leaf} but negatively correlated with VPD. The correlation between P_{max} and VPD ($r = -0.31$) was stronger than that between P_{max} and T_{leaf} ($r = 0.22$). The correlations between LMA and RDINC with P_{max} ($r = 0.77$ and $r = 0.70$ respectively) were stronger than those between T_{leaf} and VPD with P_{max} . LMA was positively correlated with P_{max} (Figure 3c), and, in contrast, RDINC was negatively correlated with P_{max} (Figure 3d). R_d was positively correlated with T_{leaf} , VPD and LMA (Figure 3e–g), but the correlation between R_d and T_{leaf} was the most significant ($r = 0.69$). In contrast, R_d was negatively correlated with RDINC (Figure 3h), which was similar to the correlation of P_{max} . $g_{\text{s-sat}}$ exhibited almost the same correlation patterns with the above factors (T_{leaf} , VPD, LMA and RDINC) (Figure 3i–l) as those of P_{max} , which indicated that $g_{\text{s-sat}}$ was closely associated with P_{max} .

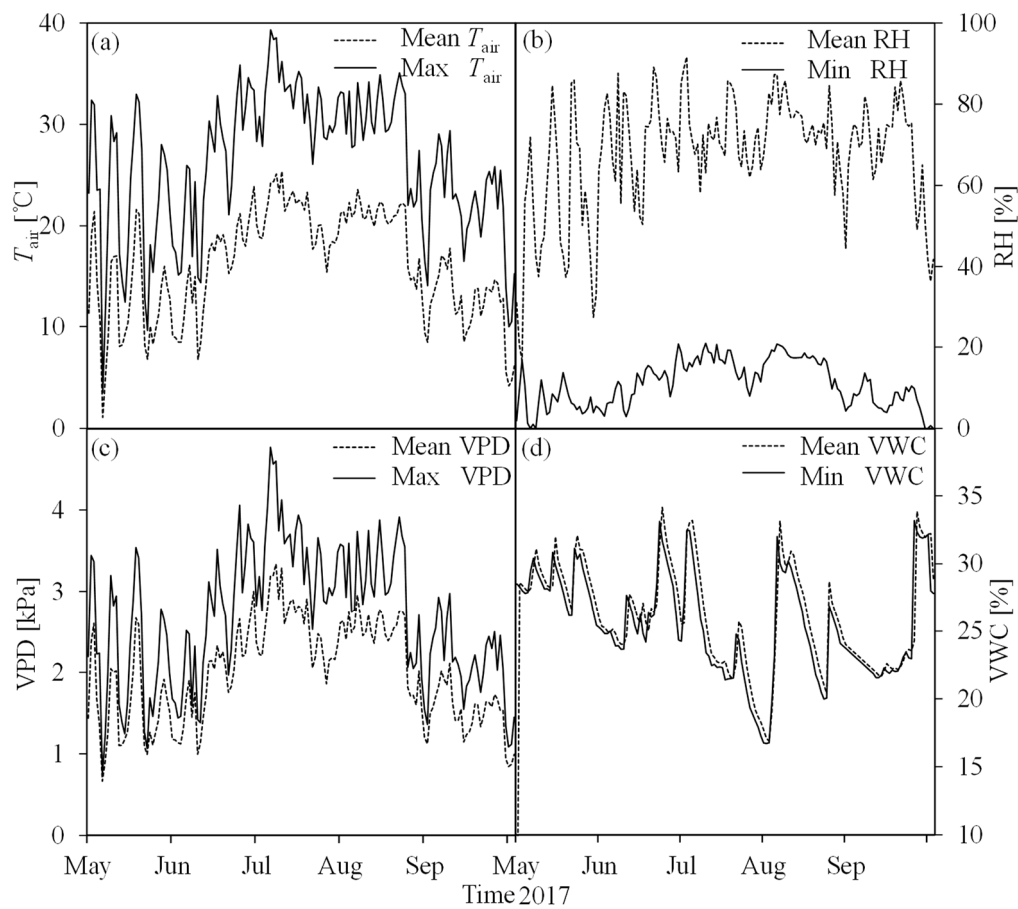


Figure 2. Seasonal course of the main environmental parameters during the period of this study (May–September 2017): (a) daily mean air temperature (mean T_{air}) and maximum air temperature (max T_{air}); (b) daily mean relative humidity (mean RH) and minimum relative air humidity (min RH); (c) daily mean vapor pressure deficit (mean VPD) and maximum vapor pressure deficit (max VPD); (d) daily mean soil moisture (mean VWC) and minimum soil moisture (min VWC).

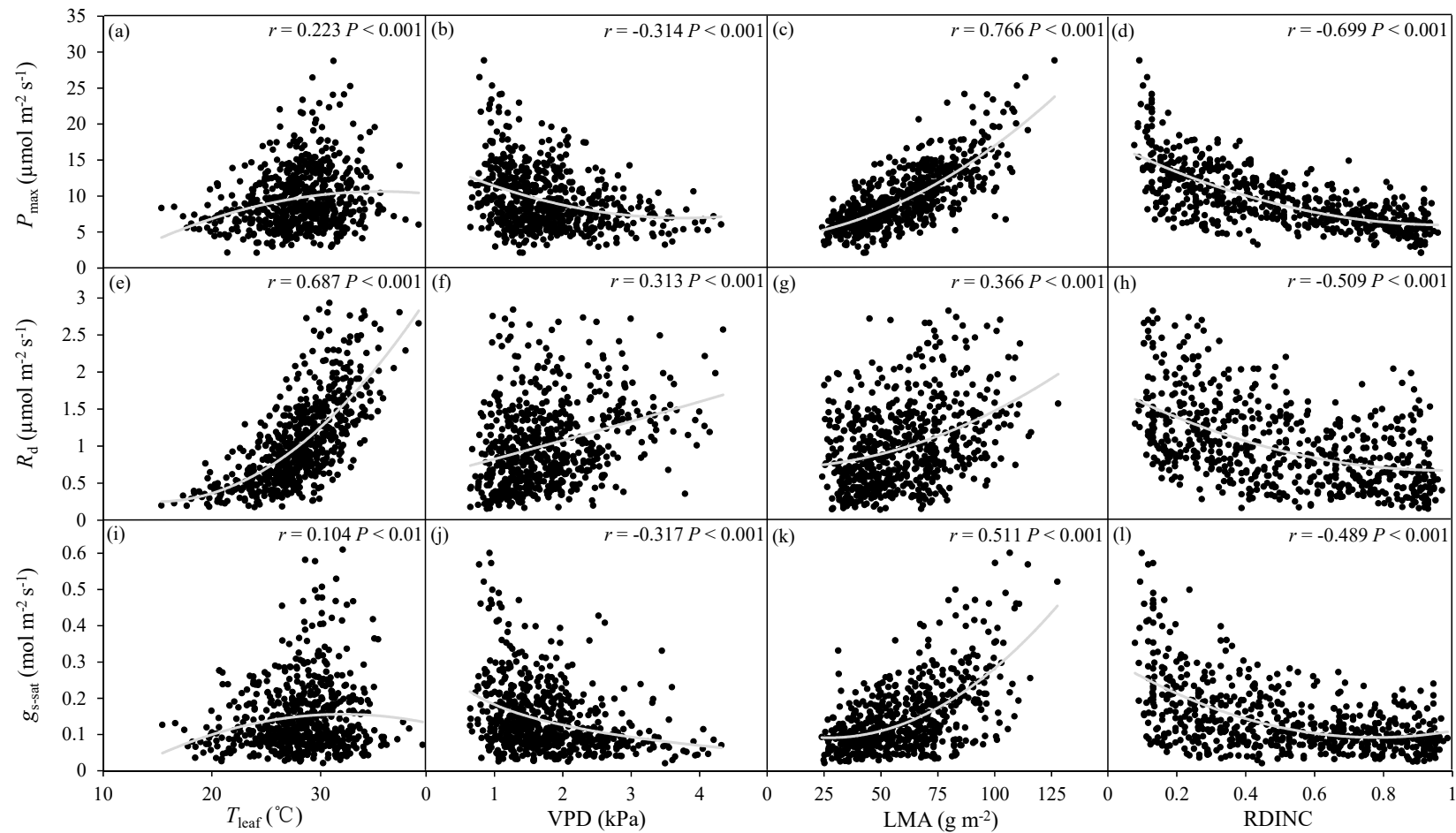


Figure 3. The relationships: (a–d) between the light-saturated net photosynthetic rate (P_{\max}) and leaf temperature (T_{leaf}), vapor pressure deficit (VPD), leaf mass per area (LMA) and relative depth into the crown (RDINC); (e–h) between dark respiration (R_d) and T_{leaf} , VPD, LMA and RDINC; (i–l) between light-saturated stomatal conductance ($g_{s\text{-sat}}$) and T_{leaf} , VPD, LMA and RDINC. The r values are Spearman's correlation coefficients. The solid gray line represents the fitting results based on polynomial equations.

3.3. Standardization of Photosynthetic Parameters

According to the relationships between P_{\max} and T_{leaf} , VPD, LMA and RDINC (Figure 3a–d), regression analysis was conducted among P_{\max} and T_{leaf} , VPD, LMA, RDINC and their combinations. Hence, the combination of LMA, VPD and RDINC was selected as the best variable for estimating P_{\max} . Thus, the P_{\max} was converted to a standard P_{\max} (SP_{\max}) using following the equation:

$$P_{\max} = a_0 + a_1 \times \ln\left(\frac{\text{LMA}}{\text{VPD} \times \text{RDINC}}\right) \quad (2)$$

where a_0 and a_1 are estimable parameters.

Similarly, regression analysis among $g_{s\text{-sat}}$ and T_{leaf} , VPD, LMA, RDINC and their combinations was also conducted. The results showed that $\ln\left(\frac{\text{LMA}}{\text{VPD} \times \text{RDINC}}\right)$ was also the best combination for estimating $g_{s\text{-sat}}$. Thus, $g_{s\text{-sat}}$ was converted to a standard $g_{s\text{-sat}}$ ($Sg_{s\text{-sat}}$) using following equation:

$$g_{s\text{-sat}} = b_0 \times \ln\left(\frac{\text{LMA}}{\text{VPD} \times \text{RDINC}}\right)^{b_1} \times b_3^{\ln\left(\frac{\text{LMA}}{\text{VPD} \times \text{RDINC}}\right)} \quad (3)$$

where b_0 , b_1 and b_2 are estimable parameters.

Previous studies showed that R_d could be estimated by the exponential function [71–75] based on the exponential correlation between R_d and T_{leaf} . In this study, R_d demonstrates a similar exponential correlation with T_{leaf} ; thus, the exponential function was applied for estimating R_d , which is described as follows:

$$R_d = c_0 \times \exp(c_1 \times T_{\text{leaf}}) \quad (4)$$

where c_0 and c_1 are estimable parameters.

As R_d was also significantly related to LMA (Figure 3g) and RDINC (Figure 3h), we divided all the R_d values into nine groups according to RDINC at intervals of 0.1 and fitted Equation (4) to each group to obtain the parameters c_0 and c_1 . Then, the relationships between c_0 and c_1 and the mean values of RDINC were analyzed (Figure 4a,b). Similarly, the R_d was also divided into 10 groups according to the LMA at intervals of 10 g m^{−2}, and the relationships between c_0 and c_1 and the mean values of LMA were analyzed (Figure 4c,d). The results showed that c_0 and c_1 were both strongly correlated with RDINC and LMA. Thus, Equation (4) was further modified by reparameterizing c_0 and c_1 using RDINC and LMA, and the modified equations were determined according to R^2 and RMSE. Then, the final R_d estimated equation was described as follows:

$$R_d = (d_0 \times \text{RDINC} + d_1) \times \exp((d_2 \times \text{LMA} + d_3) \times T_{\text{leaf}}) \quad (5)$$

where d_0 , d_1 , d_2 and d_3 are estimable parameters.

The evaluation results of the above regression Equations (2), (3) and (5) are listed in Table 3. The R^2 values of the three regression equations were above 0.5, indicating that the above regression equations could estimate the photosynthetic parameters well. According to the regression equations, SP_{\max} , SR_d and $Sg_{s\text{-sat}}$ could be obtained under any unified environmental conditions across the whole phenological phase. This could resolve the influence of the changing environment on photosynthesis, which makes analyzing the spatial and seasonal variations in the photosynthetic parameters more reasonable.

Table 3. Fitting statistics for simulations of P_{\max} , $g_{s\text{-sat}}$ and R_d .

Photosynthetic Parameters	R^2	RMSE
P_{\max} ($\mu\text{mol m}^{-2} \text{s}^{-1}$)	0.769	2.00
R_d ($\mu\text{mol m}^{-2} \text{s}^{-1}$)	0.575	0.37
$g_{s\text{-sat}}$ ($\text{mol m}^{-2} \text{s}^{-1}$)	0.546	0.06

R^2 , coefficient of determination; RMSE, the root mean square error.

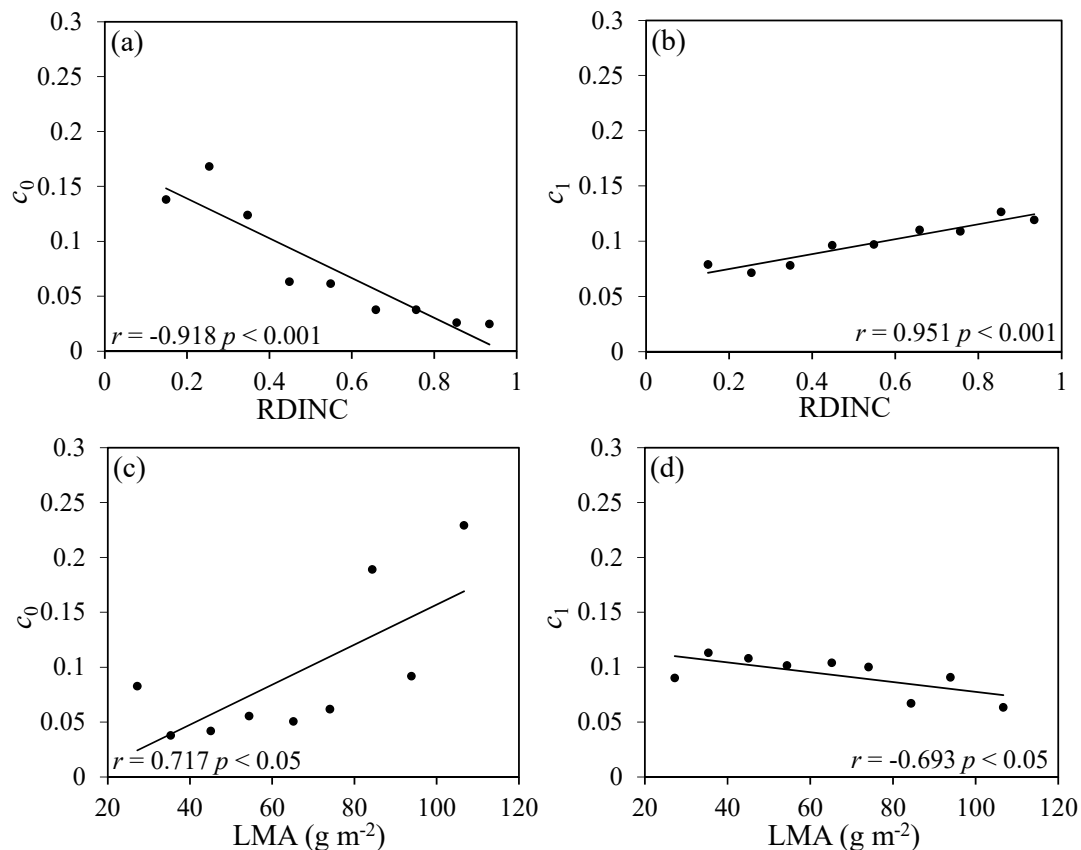


Figure 4. Relationships between the parameters (c_0 and c_1) of Equation (4) and the relative depth into the crown (RDINC): (a,b) relationship of c_0 and c_1 versus RDINC; (c,d) relationship of c_0 and c_1 versus LMA (leaf mass per area). The r values are Pearson's correlation coefficients. Solid lines are trend lines.

3.4. Vertical Profiles of Standardized and Non-Standardized Photosynthetic Parameters during the Growing Season

All three photosynthetic parameters exhibited a similar phenomenon of decreasing with the increasing RDINC throughout the growth season (Figure 5). SP_{\max} showed a similar nonlinear declining tendency with RDINC in each measured period, and the slope gradually reduced with the increase in RDINC. However, the vertical patterns of SP_{\max} still varied among the different phenological phases. The difference in SP_{\max} from treetop to bottom (DTB) was small during the early leaf-expanding phase (Figure 5(A1)) but then increased as days progressed (Figure 5(A2–A4)), finally tending to be stable until the leaf fully expanded (Figure 5(A5–A8)). The vertical pattern of non-standardized P_{\max} was different from that of SP_{\max} , especially during the leaf-expanding phase. Although SR_d reduced with the increasing RDINC across the whole growing season (Figure 5(B1–B4)), the downtrend was weaker than that of SP_{\max} . The vertical variations in the non-standardized R_d were more obvious than those of SR_d during the growing season. $Sg_{s\text{-sat}}$ exhibited a similar vertical pattern to that of SP_{\max} , but the pattern of $Sg_{s\text{-sat}}$ was more significant. Non-standardized $g_{s\text{-sat}}$ exhibited different

vertical patterns (Figure 5C) in contrast to S_{g-sat} during the growing season, with the exception of August (Figure 5(C6,C7)). The obvious seasonal variation in the vertical patterns also displayed that the DTBs increased as days went on until August.

3.5. The Response of Vertical Patterns of Standardized Photosynthetic Parameters to the Different Gradients of Environmental Conditions

According to the range of T_{leaf} during the growing season, the environmental conditions were divided into three gradients from 10 °C to 40 °C at 10 °C intervals. Then, the mean value of each gradient of T_{leaf} was taken as the representative. In addition, the corresponding VPD values of T_{leaf} were also averaged in each gradient of T_{leaf} . Finally, the environmental conditions were divided into three levels as I ($T_{leaf} = 18.7$ °C and VPD = 1.1 kPa), II ($T_{leaf} = 26.7$ °C and VPD = 1.6 kPa) and III ($T_{leaf} = 32.1$ °C and VPD = 2.2 kPa). The vertical patterns of the three standardized photosynthetic parameters (SP_{max} , SR_d and S_{g-sat}) at the above three levels of environmental conditions (I, II and III) and the non-standardized values were compared in each measured period (Figure 5).

Different gradients of environmental conditions usually showed a significant influence on the SP_{max} . The SP_{max} values at level I were, on average, 14.4% and 28.4% greater than those at levels II and III, respectively. The DTBs of P_{max} were, on average, 36.7% smaller than those of SP_{max} under the three environmental conditions (I, II and III) before August (Figure 5(A1–A5)), but then the DTBs of P_{max} were, on average, 29.6% greater than those of SP_{max} under the three environmental conditions (I, II and III) after August (Figure 5(A6–A8)). The mean SR_d across the growing seasons at level III was, on average, 3.3 times and 2.0 times greater than those at level I and level II, respectively. The mean DTBs of SR_d during the growing season were only $0.23 \mu\text{mol m}^{-2} \text{s}^{-1}$, $0.45 \mu\text{mol m}^{-2} \text{s}^{-1}$ and $0.70 \mu\text{mol m}^{-2} \text{s}^{-1}$ under the three environmental conditions (I, II and III), respectively. Different environmental conditions also had an obvious influence on vertical variations in S_{g-sat} . The mean values of S_{g-sat} at level I were, on average, 15.3% and 28.2% greater than those at levels II and III, respectively, and the mean DTBs at level I were 30.0% and 65.1% greater than those at levels II and III, respectively, during the growing season.

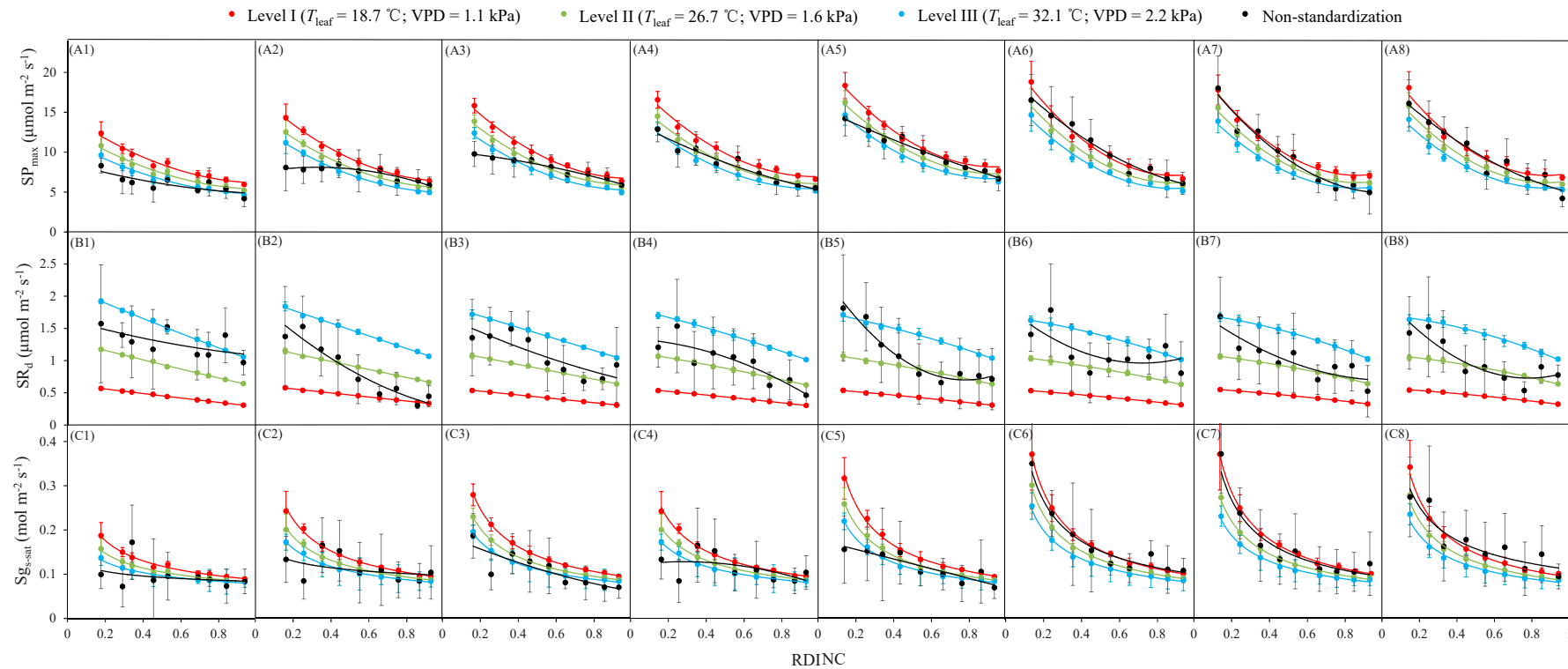


Figure 5. Vertical profiles of the standardized and nonstandardized light-saturated net photosynthetic rate (SP_{max}) (A), dark respiration (SR_d) (B) and light-saturated stomatal conductance (Sg_{s-sat}) (C) during the growing season. (1–8) represent eight measurement campaigns from 15th May to 10th September, respectively. Data points represent the mean values (solid bars represent the standard deviation) in each RDINC (relative depth into the crown) and measurement period. Solid lines are trend lines.

3.6. Seasonal Evolution of Standardized and Non-Standardized Photosynthetic Parameters during the Growing Season

The seasonal variations in SP_{max} generally demonstrated a parabolic trend during the growing season at the different RDINC values (Figure 6(A1–A9)), and this seasonal pattern of SP_{max} became increasingly obvious with the decrease in RDINC, which indicated that the responses of the leaves to phenological phases were usually more sensitive in the upper crown than in the lower crown. Obvious peaks of SP_{max} were found in early August in the upper crown ($RDINC \leq 0.3$), but there was no obvious seasonal variation in the middle and lower crown ($RDINC \geq 0.4$). Similar to the analysis of the vertical profiles of SP_{max} , the seasonal variations in SP_{max} were also analyzed. The range of SP_{max} was large in the top of the crown, but the phenomenon weakened with the increase in RDINC. The seasonal patterns of non-standardized P_{max} were significantly different from those of SP_{max} , especially in the upper part of the crown ($RDINC \leq 0.5$), e.g., the ranges of P_{max} were, on average, 2.4 times greater than those of SP_{max} , but the seasonal variations in P_{max} in the lower part of the crown ($RDINC \leq 0.5$) were not much different from those of SP_{max} , which was probably associated with the small values and weak variations in SP_{max} among the different phenological phases (Figure 6(A6–A9)). SR_d also exhibited a concave seasonal variation in contrast with SP_{max} , but the range of variation was obviously smaller than that of SP_{max} (Figure 6(B1–B9)). The seasonal variations in R_d were irregular, though there were weak negative correlations with the date of the year (DOY), which appeared when the RDINC was 0.4 (Figure 6(B4)). Sg_{s-sat} also exhibited a parabolic seasonal pattern similar to that of SP_{max} , but the phenomenon weakened with the increase in RDINC. At the bottom of the crown, the Sg_{s-sat} was almost invariable during the growing season (Figure 6(C9)). Non-standardized g_{s-sat} exhibited a positive linear correlation with DOY during the growing season, which was different from Sg_{s-sat} .

3.7. The Response of Seasonal Evolutions of Standardized Photosynthetic Parameters to the Different Gradients of Environmental Conditions

Different gradients of environmental conditions usually showed a significant influence on the seasonal patterns of photosynthetic parameters. For example, the range of SP_{max} was $7.15 \mu\text{mol m}^{-2} \text{s}^{-1}$, $6.27 \mu\text{mol m}^{-2} \text{s}^{-1}$ and $5.61 \mu\text{mol m}^{-2} \text{s}^{-1}$ at levels I, II and III, respectively, at the top of the crown (Figure 6(A1)), but then these values dropped to $1.37 \mu\text{mol m}^{-2} \text{s}^{-1}$, $1.21 \mu\text{mol m}^{-2} \text{s}^{-1}$ and $1.08 \mu\text{mol m}^{-2} \text{s}^{-1}$, respectively, at the bottom of the crown (Figure 6(A9)). The range of SP_{max} at level I fluctuated more than those at level II and level III. Similarly, different gradients of environmental conditions also significantly influenced the seasonal patterns of SR_d . The average range of SR_d in the top of the crown was $0.05 \mu\text{mol m}^{-2} \text{s}^{-1}$, $0.15 \mu\text{mol m}^{-2} \text{s}^{-1}$ and $0.31 \mu\text{mol m}^{-2} \text{s}^{-1}$ at levels I, II and III, respectively, which declined with the increasing RDINC to reach $0.01 \mu\text{mol m}^{-2} \text{s}^{-1}$, $0.03 \mu\text{mol m}^{-2} \text{s}^{-1}$ and $0.60 \mu\text{mol m}^{-2} \text{s}^{-1}$, respectively, at the bottom of the crown. The three gradients of environmental conditions strongly influenced the values of Sg_{s-sat} , especially in the upper crown, where the lower temperature and higher humidity were more favorable for gas exchange. However, in the lower crown, the difference in Sg_{s-sat} among levels I, II and III could be ignored.

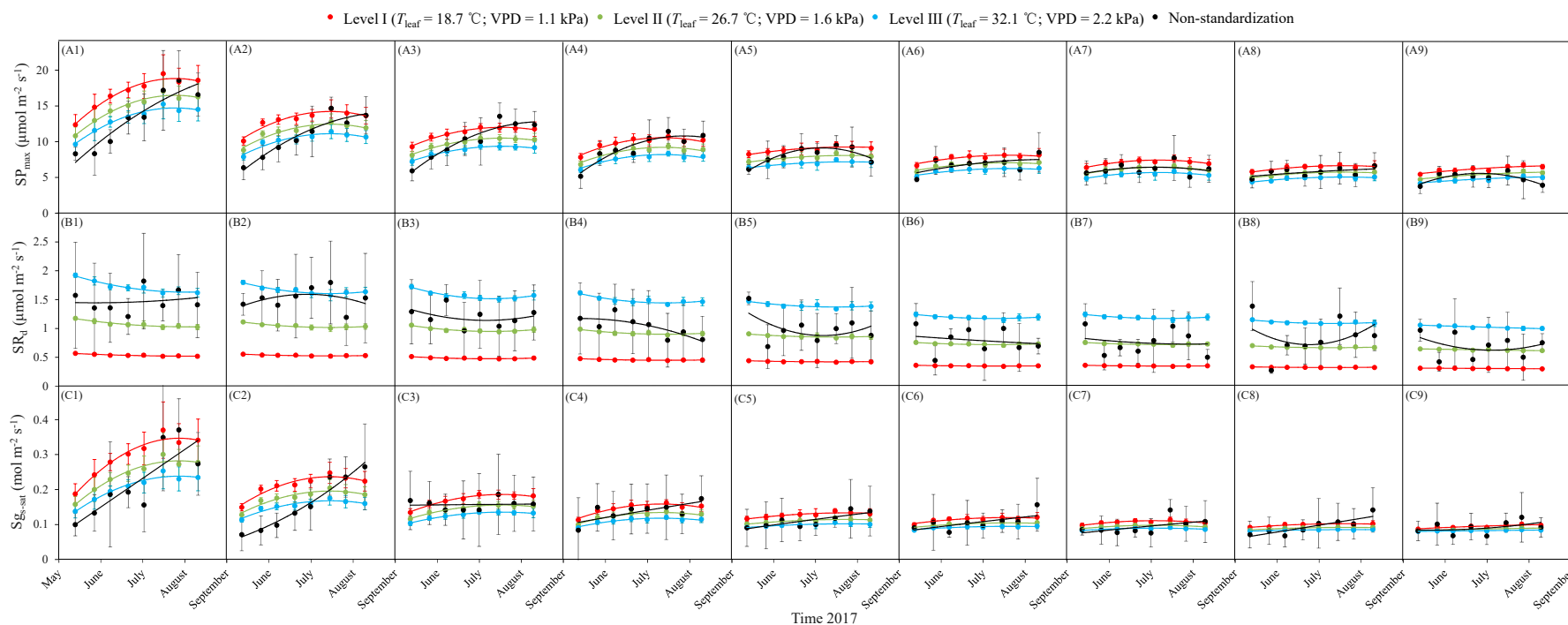


Figure 6. Seasonal evolution of standardized and nonstandardized photosynthetic parameters: **(A)** light-saturated net photosynthetic rate (SP_{max}), **(B)** dark respiration (SR_d) and **(C)** light-saturated stomatal conductance (Sg_{s-sat}) during the growing season. (1–9) represent nine vertical positions within the crown from the relative depth into the crown (RDINC) of 0.1 to 0.9, respectively, at 0.1 intervals. Data points represent the mean values (solid bars represent the standard deviation) in each RDINC and measurement period. Solid lines are trend lines.

4. Discussion

4.1. Relationships between Photosynthetic Parameters and Environmental Factors

In our study, the T_{leaf} demonstrated a parabolic correlation with P_{max} (Figure 3a), which was also found in many other studies that focused on different tree species, e.g., *Quercus crispula* Blume [68], *Picea mariana* Mill. [76], *Pinus cembra* L. [77], *Eucalyptus crebra* F.Muell. [47], *Pinus pinea* L. [78], *Quercus ilex* L. and *Juniperus oxycedrus* L. [79]. The optimal temperature for P_{max} was approximately 30 °C (Figure 3a), which was slightly higher than that indicated in other studies [78,80]. This was probably because the highest P_{max} values appeared in July and August, whose mean temperatures were significantly higher than those of the other months (Figure 2a). Hikosaka et al. [81] obtained a similar result and found that the optimal temperature of P_{max} increased with increasing ambient temperature. VPD exhibited a significant negative correlation with P_{max} (Figure 3b), which was associated with the response of g_s to the high VPD [81]. This phenomenon was more obvious in the upper crown (not shown), which was presumably because the leaves in the upper crown are more frequently exposed to environmental stresses, and the variations in VPD in the upper crown are more sensitive and larger [51]. R_d exhibited a typical exponential relationship with T_{leaf} , and the correlation coefficient was as high as 0.69 (Figure 3e), which indicated that T_{leaf} was the main environmental factor affecting the R_d , though VPD also demonstrated a significant correlation with R_d (Figure 3f). This is in line with other studies [72,73,77,80,82–85]. $g_{s\text{-sat}}$ has been reported to be highly related to P_{max} [28], especially in drier periods. The $g_{s\text{-sat}}$ was actually the most limiting process to photosynthesis [54]; thus, it generally exhibited a high correlation with P_{max} . In our study, the correlation coefficient between $g_{s\text{-sat}}$ and P_{max} reached 0.76, and $g_{s\text{-sat}}$ exhibited similar relationships with T_{leaf} and VPD to those of P_{max} (Figure 3i,j). Higher temperature and VPD usually reduced the $g_{s\text{-sat}}$, which was also the main reason causing the decline of P_{max} at high temperatures and VPD values [81,86].

4.2. Relationships between Photosynthetic Parameters and LMA

Our results showed that P_{max} demonstrated a significant and positive correlation with LMA (Figure 3d), which is in accordance with previous research [21,22,87]. Bond et al. [11] even simulated the P_{max} by a linear regression between P_{max} and LMA. In contrast, Han [3] found a negative relationship between P_{max} and LMA for *Pinus densiflora* Seib. et Zucc., which was probably associated with the higher LMA values (greater than 200 g m⁻²) than those in our study (less than 130 g m⁻²). Similar results have been reported previously, but most of these reports concerned tall tree species [17,54,80,81], and all of them demonstrated negative relationships between P_{max} and LMA. Previous investigations suggested that LMA was closely associated with mesophyll conductivity to carbon dioxide [3,26], which consequently influences leaf photosynthesis [24,27,28]. Therefore, we speculated that the relatively low LMA in our study might not sufficiently limit the mesophyll conductivity to carbon dioxide and further restrict P_{max} . In other studies of larch species, the LMA values were similar to our results. Mitamura et al. [88] suggested that the mean LMA of young (16–20 years old) *Larix decidua* Mill. was approximately 134 g m⁻². Fellner et al. [49] and Kurachi et al. [64] also obtained low LMA values (less than 100 g m⁻²) in studies of young *Larix decidua* and *Larix leptolepis* Siebold & Zucc., respectively. R_d has been reported to be positively related to LMA in other studies [72,83,85], but their correlation was usually weaker. Our result also showed a slightly positive correlation between R_d and LMA ($r = 0.37$, Figure 3g). However, we speculated that the significant correlation between R_d and LMA was not real. This result was probably associated with the stronger correlation between LMA and RDINC (Figure 7a). $g_{s\text{-sat}}$ also exhibited a high positive correlation with LMA (Figure 3k) to that of P_{max} . In our opinion, stomatal movement is a sensitive response of leaves to changes in the external environment. Thus, the significant correlation between $g_{s\text{-sat}}$ and LMA was an indirect relationship that depended on the plasticity of LMA to the environment [89–91].

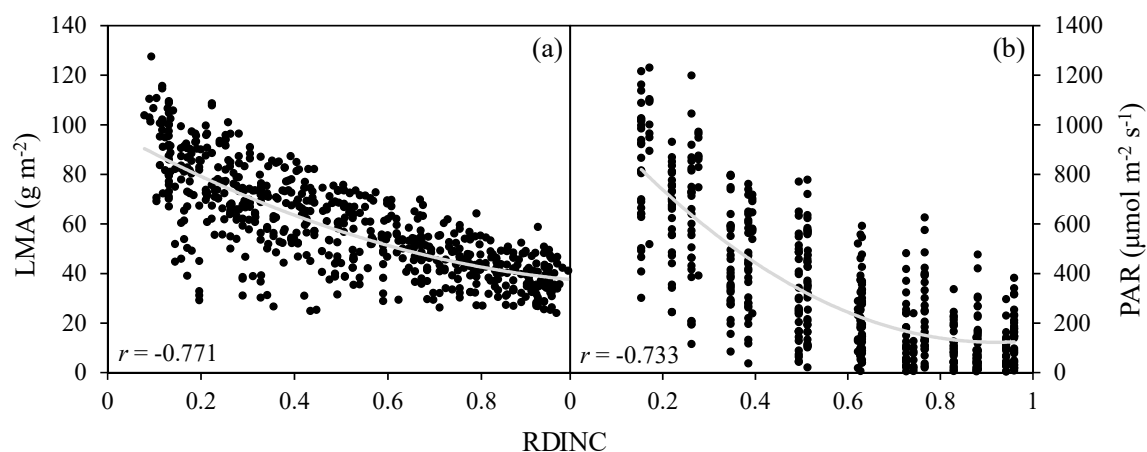


Figure 7. The relationships: (a) between leaf mass per area (LMA) and relative depth into the crown (RDINC) and (b) between photosynthetically active radiation (PAR) and RDINC. The r values are Spearman's correlation coefficients. The solid gray line represents the fitting results based on polynomial equations.

4.3. Standardization of Photosynthetic Parameters

In our study, the high forest density (averagely 2800 trees hm^{-2}) led to an obvious spatial variation in the microenvironment within the crown. In addition, the typical midlatitude continental monsoon climate and mountainous landforms of the experimental area resulted in abrupt and frequent weather variations at diurnal and monthly scales throughout the entire growing seasons (Figure 2). Both of the above conditions made it more difficult to control the environmental conditions at consistent levels among all measurements. Thus, we analyzed the relationships between the major photosynthetic parameters (P_{\max} , R_d and $g_{s\text{-sat}}$) and environmental factors (T_{leaf} and VPD), a morphological factor (LMA), the vertical position within the crown (RDINC) and their combinations to determine the rules of leaf photosynthesis response to the above factors. According to the high correlation between P_{\max} and LMA, VPD and RDINC, the P_{\max} was estimated by their combinations (Equation (2)), and the R^2 value was as high as 0.77 (Table 3), which indicated that the equation fitted P_{\max} well. Bond et al. [11] suggested that P_{\max} could be estimated well only by LMA. Similar to the procedure for P_{\max} , we also established a regression equation for R_d according to the relationships between this value and other factors. As confirmed by many reports, R_d could be estimated well by the exponential function [71–74]. Some previous studies even reported that R_d could be well estimated only by LMA [84,85]. In our study, R_d exhibited a similar exponential correlation with T_{leaf} (Figure 3e). Furthermore, we found that R_d also exhibited significant correlations with RDINC and LMA (Figure 3h,g). Thus, further reparameterization was conducted by incorporating RDINC and LMA into the exponential function. Finally, R_d was well estimated ($R^2 = 0.58$, Table 3) by the modified exponential function (Equation (5)). As $g_{s\text{-sat}}$ was highly correlated with P_{\max} , $g_{s\text{-sat}}$ also exhibited a strong correlation with the combination of LMA, VPD and RDINC (LMA/VPD/RDINC), but their relationship was closer to nonlinear rather than linear. Thus, $g_{s\text{-sat}}$ was estimated by a nonlinear form (Equation (3)), and the R^2 value was also greater than 0.5 (Table 3). Finally, P_{\max} , R_d and $g_{s\text{-sat}}$ were standardized into SP_{\max} , SR_d and $\text{Sg}_{s\text{-sat}}$, respectively, when the spatial and seasonal variations were analyzed to avoid the influence of the changeable environment.

4.4. Spatial Variation in Standardized Leaf Photosynthetic Parameters

Our results reported above illustrated that SP_{\max} decreased obviously from treetop to bottom (Figure 5(A1–A9)), which is consistent with other studies [1,4,11,65,73]. The SR_d was also negatively correlated with RDINC (Figure 5(B1–B8)), as already documented for different species [1,27,52,65,83,92]. The vertical patterns of both SP_{\max} and SR_d indicated that the metabolic capacity was higher in the

upper crown than in the lower crown [72]. The vertical patterns of SP_{max} and SR_d were similar to the vertical distribution of PAR (Figure 7b), which further indicated that light acclimation plays an important role in the vertical variation of photosynthesis in short trees. Different gradients of environmental conditions obviously influenced the vertical patterns of SP_{max} and SR_d . The DTBs of SP_{max} and Sg_{s-sat} were respectively reduced by 21.6% and 38.9% on average when the environmental conditions varied from level I ($T_{leaf} = 18.7\text{ }^{\circ}\text{C}$ and $VPD = 1.1\text{ kPa}$) to level III ($T_{leaf} = 32.1\text{ }^{\circ}\text{C}$ and $VPD = 2.2\text{ kPa}$) (Figure 5A), but the DTB of SR_d increased by 1.6-fold on average with the same change in environmental conditions (Figure 5B). The pronounced differences in the vertical patterns of SP_{max} and SR_d among the different gradients of environmental conditions implied that focusing on only a single environmental condition could not accurately reveal the vertical rules of SP_{max} , SR_d and Sg_{s-sat} in all environmental gradients. The vertical patterns of SP_{max} also exhibited obvious seasonal variations under the same environmental conditions. The DTB was smaller in the early leaf-expansion period (Figure 5(A1)), then increased during the leaf-expanding period (Figure 5(A1–A5)), and finally tended to remain stable. This reflected that the photosynthetic capacity in the upper crown usually increased faster than that in the lower crown during the growing season. The vertical patterns of SR_d also demonstrated obvious differences among the different periods, and the DTB declined as the growth season progressed. The difference in SR_d among different environmental conditions was $0.58\text{ }\mu\text{mol m}^{-2}\text{ s}^{-1}$ on average across the growing seasons, which was slightly greater than that among different vertical positions ($0.46\text{ }\mu\text{mol m}^{-2}\text{ s}^{-1}$ on average). This implied that environmental conditions and vertical position within the crown were both main factors influencing the SR_d . The seasonal difference of the vertical patterns of Sg_{s-sat} was similar to that of SP_{max} , but the difference among different environmental conditions was much smaller in the bottom of the crown than in the top of the crown. In summary, the vertical patterns of the unstandardized photosynthetic indicators were significantly different from the standardized photosynthetic indicators, which indicated that standardization is important before analyzing the vertical variation in photosynthesis. In addition, the obvious difference in the vertical patterns of standardized photosynthetic indicators among different growing periods implied that the phenological phase should also be considered when analyzing the vertical variation in photosynthesis.

4.5. Seasonal Variations in Standardized Leaf Photosynthetic Parameters

In this study, the seasonal variation in SP_{max} generally demonstrated a similar parabolic profile during the growing season (Figure 6(A1–A9)), in accordance with previous reports [26,31–33,56,72,76,87,93]. At the leaf-spreading phase, the increasing SP_{max} was the result of a gradual increase in photosynthetic capacity [32]. However, during the leaf senescence phase, the decreasing SP_{max} was associated with the decrease in mesophyll conductivity to carbon dioxide caused by increasing sizes of chloroplasts, starch granules and plastoglobuli [26] and the resorption of nitrogen [93]. The highest SP_{max} value appeared in early August, which was accompanied by a recovery of soil moisture (VWC) from very low values (16.7%, Figure 2d). Thus, we speculate that a short-term drought may cause a sharp rebound of leaf physiological properties when the drought disappears. Similar results have also been reported in other studies [32,38,80]. The changes in seasonal patterns with RDINC indicated that the response of SP_{max} to the growing period was more sensitive in the upper crown than in the lower crown. Different gradients of VPD also led to different responses of SP_{max} to growing periods, and lower VPD usually caused more abrupt seasonal variations in SP_{max} than did high VPD.

Previous research has suggested that the seasonal variation in R_d is mainly driven by the seasonal patterns of temperature and LMA [72,83,84]. It is well known that starch and soluble sugars are the main reactants of the respiratory process; thus, their contents directly impact respiration. At the same time, temperature also indirectly limited respiration by affecting the activities of enzymes that participate in respiration. However, in the early period of leaf expansion, R_d generally exhibited the highest value across the entire growing season, which was not mainly dependent on temperature

and LMA [94]. It has been confirmed that the reduction of the leaf-expansion phase is due to the decrease in cytochrome mediation [95]. The seasonal patterns of SR_d were close to a concave curve in the upper crown when the environmental condition was at level I (Figure 6(B1–B4)), which followed a similar trajectory to those found in other investigations [92,94,96]. However, in the middle and lower crown, the seasonal variations in SR_d were not significant (Figure 6(B5–B9)), which indicated that the response of SR_d to the growing period was more sensitive in the upper crown than in the lower crown. When the environmental condition was at level II and level III, the seasonal variations in SR_d were weaker than that at level I. The different seasonal variations of SR_d under different environments further reflected that a single environmental condition could not accurately reveal the seasonal rules of SR_d across all environmental gradients. Sg_{s-sat} usually exhibited similar seasonal patterns to those of SP_{max} [8] because they were highly correlated. However, Sg_{s-sat} demonstrated a more sensitive response to the different environmental conditions in the top of the crown but was very insensitive in the lower crown. This result was probably caused by the acclimatization of needles in the different microenvironments [51]. The seasonal patterns of all of the photosynthetic indicators gradually weakened with the increase in RDINC, which indicated that the vertical difference should also be considered when analyzing the seasonal variations in photosynthesis.

5. Conclusions

In our study, P_{max} , R_d and g_{s-sat} were standardized to SP_{max} , SR_d and Sg_{s-sat} according to the relationships between them and with representative environmental factors (T_{leaf} and VPD), a morphological characteristic (LMA) and the spatial index (RDINC). For *Larix olgensis*, SP_{max} , SR_d and Sg_{s-sat} exhibited a similar vertical pattern that decreased with the increase in RDINC. The vertical differences in SP_{max} and Sg_{s-sat} became more obvious after the needles fully expanded, but the vertical differences in SR_d did not vary significantly with the growing phases. The seasonal patterns of SP_{max} and Sg_{s-sat} tended to be parabolic, and this tendency was more obvious in the upper crown. By contrast, the seasonal pattern of SR_d was a concave curve. Both of the spatial and seasonal variations exhibited significant differences among different gradients of environmental conditions. Under the condition of high temperature and low humidity, the photosynthesis of needles was generally inhibited; however, the condition of high temperature is usually beneficial to the respiration. This may explain the common phenomenon of midday depression of photosynthesis. In addition, this phenomenon was more obvious in the top of the crown. These results implied that a single environmental condition could not accurately reveal the spatial or seasonal rules of all gradients of environmental conditions. Thus, standardization was necessary before analyzing the spatial and seasonal variations in photosynthesis. Neither the spatial pattern nor the seasonal pattern of the photosynthetic indicators was static, and they were closely related to each other. Thus, we suggest that the spatial and seasonal variations in photosynthetic indicators should be analyzed at the same time.

Author Contributions: Q.L. undertook data analysis and wrote most of the paper. F.L. supervised and coordinated the research paper, designed and installed the experiment, made some measurements, and contributed to the writing of the paper.

Funding: This research was financially supported by the National Key R & D Program of China (No. 2017YFD0600402).

Acknowledgments: The authors would like to thank Xiankui Quan for valuable advice and Xingchang Wang, Longfei Xie, Xiang Li, Fanlin Kong and Yibo Sun who provided and collected the data for this study. We would like to express our appreciation to three anonymous reviewers for their constructive comments on the manuscript.

Conflicts of Interest: The authors declare no conflict of interest.

References

1. O'Grady, A.P.; Worledge, D.; Wilkinson, A.; Battaglia, M. Photosynthesis and respiration decline with light intensity in dominant and suppressed *Eucalyptus globulus* canopies. *Funct. Plant Biol.* **2008**, *35*, 439–447. [CrossRef]

2. Cavaleri, M.A.; Oberbauer, S.F.; Clark, D.B.; Clark, D.A.; Ryan, M.G. Height is more important than light in determining leaf morphology in a tropical forest. *Ecology* **2010**, *91*, 1730–1739. [[CrossRef](#)] [[PubMed](#)]
3. Han, Q.M. Height-related decreases in mesophyll conductance, leaf photosynthesis and compensating adjustments associated with leaf nitrogen concentrations in *Pinus densiflora*. *Tree Physiol.* **2011**, *31*, 976–984. [[CrossRef](#)] [[PubMed](#)]
4. Kosugi, Y.; Takanashi, S.; Yokoyama, N.; Kamakura, M. Vertical variation in leaf gas exchange parameters for a Southeast Asian tropical rainforest in Peninsular Malaysia. *J. Plant Res.* **2012**, *125*, 735–748. [[CrossRef](#)] [[PubMed](#)]
5. Leuning, R.; Kelliher, F.M.; De Pury, D.G.G.; Schulze, E.D. Leaf nitrogen, photosynthesis, conductance and transpiration: Scaling from leaves to canopies. *Plant Cell Environ.* **1995**, *18*, 1183–1200. [[CrossRef](#)]
6. Oliver, C.D.; Larson, B.C. *Forest Stand Dynamics*; John Wiley & sons, Inc.: New York, NY, USA, 1996.
7. Li, F.R.; Wang, Z.F.; Wang, B.S. Studies on the effective crown development of *Larix olgensis* (I)—determination of the effective crown. *J. Northeast For. Univ.* **1996**, *24*, 1–8. (In Chinese)
8. Xu, L.; Baldocchi, D.D. Seasonal trends in photosynthetic parameters and stomatal conductance of blue oak (*Quercus douglasii*) under prolonged summer drought and high temperature. *Tree Physiol.* **2003**, *23*, 865–877. [[CrossRef](#)] [[PubMed](#)]
9. Lam, F.; Barrett, J.D.; Nakajima, S. Influence of knot area ratio on the bending strength of Canadian Douglas fir timber used in Japanese post and beam housing. *J. Wood Sci.* **2005**, *51*, 18–25. [[CrossRef](#)]
10. Bond, B.J.; Farnsworth, B.T.; Coulombe, R.A.; Winner, W.E. Foliage physiology and biochemistry in response to light gradients in conifers with varying shade tolerance. *Oecologia* **1999**, *120*, 183–192. [[CrossRef](#)] [[PubMed](#)]
11. Borghetti, M.; Vendramin, G.G.; Giannini, R. Specific leaf area and leaf area index distribution in a young Douglas. *Can. J. For. Res.* **1986**, *16*, 1283–1288. [[CrossRef](#)]
12. Cescatti, A.; Zorer, R. Structural acclimation and radiation regime of silver fir (*Abies alba* Mill.) shoots along a light gradient. *Plant Cell Environ.* **2003**, *26*, 429–442. [[CrossRef](#)]
13. Wyka, T.P.; Oleksyn, J.; Żytkowiak, R.; Karolewski, P.; Jagodziński, A.M.; Reich, P.B. Responses of leaf structure and photosynthetic properties to intra-canopy light gradients: A common garden test with four broadleaf deciduous angiosperm and seven evergreen conifer tree species. *Oecologia* **2012**, *170*, 11–24. [[CrossRef](#)] [[PubMed](#)]
14. Coble, A.P.; Cavaleri, M.A. Light drives vertical gradients of leaf morphology in a sugar maple (*Acer saccharum*) forest. *Tree Physiol.* **2014**, *34*, 146–158. [[CrossRef](#)] [[PubMed](#)]
15. Bond, B.J. Age-related changes in photosynthesis of woody plants. *Trends Plant Sci.* **2000**, *5*, 349–353. [[CrossRef](#)]
16. Ishii, H.; Ford, E.D.; Boscolo, M.E.; Manriquez, A.C.; Wilson, M.E.; Hinckley, T.M. Variation in specific needle area of old-growth Douglas-fir in relation to needle age, within-crown position and epicormic shoot production. *Tree Physiol.* **2002**, *22*, 31–40. [[CrossRef](#)] [[PubMed](#)]
17. Koch, G.W.; Sillett, S.C.; Jennings, G.M.; Davis, S.D. The limits to tree height. *Nature* **2004**, *428*, 851–854. [[CrossRef](#)] [[PubMed](#)]
18. Oldham, A.R.; Sillett, S.C.; Tomescu, A.M.F.; Koch, G. The hydrostatic gradient, not light availability, drives height-related variation in *Sequoia sempervirens* (Cupressaceae) leaf anatomy. *Am. J. Bot.* **2010**, *97*, 1087–1097. [[CrossRef](#)] [[PubMed](#)]
19. Coble, A.P.; Vanderwall, B.; Mau, A.; Cavaleri, M. How vertical patterns in leaf traits shift seasonally and the implications for modeling canopy photosynthesis in a temperate deciduous forest. *Tree Physiol.* **2016**, *36*, 1077–1091. [[CrossRef](#)] [[PubMed](#)]
20. Field, C. Allocating leaf nitrogen for the maximization of carbon gain: Leaf age as a control on the allocation program. *Oecologia* **1983**, *56*, 341–347. [[CrossRef](#)] [[PubMed](#)]
21. Kenzo, T.; Ichie, T.; Watanabe, Y.; Yoneda, R.; Ninomiya, I.; Koike, T. Changes in photosynthesis and leaf characteristics with tree height in five dipterocarp species in a tropical rain forest. *Tree Physiol.* **2006**, *26*, 865–873. [[CrossRef](#)] [[PubMed](#)]
22. Meinzer, F.C.; Bond, B.J.; Karanian, J.A. Biophysical constraints on leaf expansion in a tall conifer. *Tree Physiol.* **2008**, *28*, 197–206. [[CrossRef](#)] [[PubMed](#)]
23. Woodruff, D.R.; Meinzer, F.C.; Lachenbruch, B.; Johnson, D.M. Coordination of leaf structure and gas exchange along a height gradient in a tall conifer. *Tree Physiol.* **2009**, *29*, 261–272. [[CrossRef](#)] [[PubMed](#)]

24. Woodruff, D.R. The impacts of water stress on phloem transport in Douglas-fir trees. *Tree Physiol.* **2014**, *34*, 5–14. [[CrossRef](#)] [[PubMed](#)]
25. Benomar, L.; DesRochers, A.; Larocque, G.R. Changes in specific leaf area and photosynthetic nitrogen-use efficiency associated with physiological acclimation of two hybrid poplar clones to intraclonal competition. *Can. J. For. Res.* **2011**, *41*, 1465–1476. [[CrossRef](#)]
26. Riikonen, J.; Oksanen, E.; Peltonen, P.; Holopainen, T.; Vapaavuori, E. Seasonal variation in physiological characteristics of two silver birch clones in the field. *Can. J. For. Res.* **2003**, *33*, 2164–2176. [[CrossRef](#)]
27. Mullin, L.P.; Sillett, S.C.; Koch, G.; Tu, K.; Antoine, M.E. Physiological consequences of height-related morphological variation in *Sequoia sempervirens* foliage. *Tree Physiol.* **2009**, *29*, 1–12. [[CrossRef](#)] [[PubMed](#)]
28. Flexas, J.; Barbour, M.M.; Brendel, O.; Cabrera, H.M.; Carriqui, M.; Díaz-Espejo, A.; Douthe, C.; Dreyer, E.; Ferrio, J.P.; Gago, J.; et al. Mesophyll diffusion conductance to CO₂: An unappreciated central player in photosynthesis. *Plant Sci.* **2012**, *193*, 70–84. [[CrossRef](#)] [[PubMed](#)]
29. Grassi, G.; Vicinelli, E.; Ponti, F.; Cantoni, L.; Magnani, F. Seasonal and interannual variability of photosynthetic capacity in relation to leaf nitrogen in a deciduous forest plantation in northern Italy. *Tree Physiol.* **2005**, *25*, 349–360. [[CrossRef](#)] [[PubMed](#)]
30. Strand, M.; Lundmark, T.; Söderbergh, I.; Mellander, P.E. Impacts of seasonal air and soil temperatures on photosynthesis in Scots pine trees. *Tree Physiol.* **2002**, *22*, 839–847. [[CrossRef](#)] [[PubMed](#)]
31. Awada, T.; Radoglou, K.; Fotelli, M.N.; Constantinidou, H.I.A. Ecophysiology of seedlings of three Mediterranean pine species in contrasting light regimes. *Tree Physiol.* **2003**, *23*, 33–41. [[CrossRef](#)] [[PubMed](#)]
32. Letts, M.G.; Phelan, C.A.; Johnson, D.R.E.; Rood, S. Seasonal photosynthetic gas exchange and leaf reflectance characteristics of male and female cottonwoods in a riparian woodland. *Tree Physiol.* **2008**, *28*, 1037–1048. [[CrossRef](#)] [[PubMed](#)]
33. Wyka, T.P.; Żytkowiak, R.; Oleksyn, J. Seasonal dynamics of nitrogen level and gas exchange in different cohorts of Scots pine needles: A conflict between nitrogen mobilization and photosynthesis? *Eur. J. For. Res.* **2016**, *135*, 483–493. [[CrossRef](#)]
34. Misson, L.; Tu, K.P.; Boniello, R.A.; Goldstein, A.H. Seasonality of photosynthetic parameters in a multi-specific and vertically complex forest ecosystem in the Sierra Nevada of California. *Tree Physiol.* **2006**, *26*, 729–741. [[CrossRef](#)] [[PubMed](#)]
35. Nouvellon, Y.; Laclau, J.P.; Epron, D.; Kinana, A.; Mabiala, A.; Roupsard, O.; Bonnefond, J.M.; Maire, G.I.; Marsden, C.; Bontemps, J.D.; et al. Within-stand and seasonal variations of specific leaf area in a clonal Eucalyptus plantation in the Republic of Congo. *For. Ecol. Manag.* **2010**, *259*, 1796–1807. [[CrossRef](#)]
36. Li, J.Y.; Ou-lee, T.M.; Raba, R.; Amundson, R.G.; Last, R.L. Arabidopsis flavonoid mutants are hypersensitive to UV-B irradiation. *Plant Cell* **1993**, *5*, 171–179. [[CrossRef](#)] [[PubMed](#)]
37. Coble, A.P.; Cavaleri, M.A. Light acclimation optimizes leaf functional traits despite height-related constraints in a canopy shading experiment. *Oecologia* **2015**, *177*, 1131–1143. [[CrossRef](#)] [[PubMed](#)]
38. Pardos, M.; Puértolas, J.; Madrigal, G.; Garriga, E.; Blas, S.D.; Calama, R. Seasonal changes in the physiological activity of regeneration under a natural light gradient in a *Pinus pinea* regular stand. *For. Syst.* **2010**, *19*, 367–380. [[CrossRef](#)]
39. Craven, D.; Dent, D.; Braden, D.; Ashton, M.S.; Berlyn, G.P.; Hall, J.S. Seasonal variability of photosynthetic characteristics influences growth of eight tropical tree species at two sites with contrasting precipitation in Panama. *For. Ecol. Manag.* **2011**, *261*, 1643–1653. [[CrossRef](#)]
40. Li, C.; Xu, G.; Zang, R.; Korpelainen, H.; Berninger, F. Sex-related differences in leaf morphological and physiological responses in *Hippophae rhamnoides* along an altitudinal gradient. *Tree Physiol.* **2007**, *27*, 399–406. [[CrossRef](#)] [[PubMed](#)]
41. Wilson, K.B.; Baldocchi, D.D.; Hanson, P.J. Leaf age affects the seasonal pattern of photosynthetic capacity and net ecosystem exchange of carbon in a deciduous forest. *Plant Cell Environ.* **2001**, *24*, 571–583. [[CrossRef](#)]
42. Tanaka, K.; Kosugi, Y.; Nakamura, A. Impact of leaf physiological characteristics on seasonal variation in CO₂, latent and sensible heat exchanges over a tree plantation. *Agric. For. Meteorol.* **2002**, *114*, 103–122. [[CrossRef](#)]
43. Kosugi, Y.; Shibata, S.; Kobashi, S. Parameterization of the CO₂ and H₂O gas exchange of several temperate deciduous broad-leaved trees at the leaf scale considering seasonal changes. *Plant Cell Environ.* **2003**, *26*, 285–301. [[CrossRef](#)]

44. Esprey, L.J.; Sands, P.J.; Smith, C.W. Understanding of 3-PG using a sensitivity analysis. *For. Ecol. Manag.* **2004**, *193*, 235–250. [[CrossRef](#)]
45. Stape, J.L.; Ryan, M.G.; Binkley, D. Testing the utility of the 3-PG model for growth of *Eucalyptus grandis* × *urophylla* with natural and manipulated supplies of water and nutrients. *For. Ecol. Manag.* **2004**, *193*, 219–234. [[CrossRef](#)]
46. Davidson, R.; Mauffette, Y.; Gagnon, D. Light requirements of seedlings: A method for selecting tropical trees for plantation forestry. *Basic Appl. Ecol.* **2002**, *3*, 209–220. [[CrossRef](#)]
47. Lin, Y.S.; Medlyn, B.E.; Ellsworth, D.S. Temperature responses of leaf net photosynthesis: The role of component processes. *Tree Physiol.* **2012**, *32*, 219–231. [[CrossRef](#)] [[PubMed](#)]
48. Craven, D.; Braden, D.; Ashton, M.S.; Berlyn, G.P.; Wishnie, M.; Dent, D. Between and within-site comparisons of structural and physiological characteristics and foliar nutrient content of 14 tree species at a wet, fertile site and a dry, infertile site in Panama. *For. Ecol. Manag.* **2007**, *238*, 335–346. [[CrossRef](#)]
49. Fellner, H.; Dirnberger, G.F.; Sterba, H. Specific leaf area of European Larch (*Larix decidua* Mill.). *Trees* **2016**, *30*, 1237–1244. [[CrossRef](#)] [[PubMed](#)]
50. Bauerle, W.L.; Oren, R.; Way, D.A.; Qian, S.S.; Stoy, P.C.; Thornton, P.E.; Bowden, J.D.; Hoffman, F.M.; Reynolds, R.F. Photoperiodic regulation of the seasonal pattern of photosynthetic capacity and the implications for carbon cycling. *Proc. Nat. Acad. Sci. USA* **2012**, *109*, 8612–8617. [[CrossRef](#)] [[PubMed](#)]
51. Han, Q.; Kawasaki, T.; Katahata, S.; Mukai, Y.; Chiba, Y. Horizontal and vertical variations in photosynthetic capacity in a *Pinus densiflora* crown in relation to leaf nitrogen allocation and acclimation to irradiance. *Tree Physiol.* **2003**, *23*, 851–857. [[CrossRef](#)] [[PubMed](#)]
52. Ambrose, A.R.; Sillett, S.C.; Dawson, T.E. Effects of tree height on branch hydraulics, leaf structure and gas exchange in California redwoods. *Plant Cell Environ.* **2009**, *32*, 743–757. [[CrossRef](#)] [[PubMed](#)]
53. Rascher, U.; Bobich, E.G.; Lin, G.H.; Walter, A.; Morris, T.J.; Naumann, M.; Nichol, C.J.; Pierce, D.; Bil, K.; Kudryarov, V.N.; et al. Functional diversity of photosynthesis during drought in a model tropical rainforest—the contributions of leaf area, photosynthetic electron transport and stomatal conductance to reduction in net ecosystem carbon exchange. *Plant Cell Environ.* **2004**, *27*, 1239–1256. [[CrossRef](#)]
54. Broeckx, L.S.; Fichot, R.; Verlinden, M.S.; Ceulemans, R. Seasonal variations in photosynthesis, intrinsic water-use efficiency and stable isotope composition of poplar leaves in a short-rotation plantation. *Tree Physiol.* **2014**, *34*, 701–715. [[CrossRef](#)] [[PubMed](#)]
55. Franco, A.C. Seasonal patterns of gas exchange, water relations and growth of *Roupala montana*, an evergreen savanna species. *Plant Ecol.* **1998**, *136*, 69–76. [[CrossRef](#)]
56. Corcuera, L.; Morales, F.; Abadía, A.; Pelegrín, G. Seasonal changes in photosynthesis and photoprotection in a *Quercus ilex* subsp. *ballota* woodland located in its upper altitudinal extreme in the Iberian Peninsula. *Tree Physiol.* **2005**, *25*, 599–608. [[PubMed](#)]
57. Zhu, J.J.; Liu, Z.G.; Wang, H.X.; Yan, Q.L.; Fang, H.Y.; Hu, L.; Yu, L.Z. Effects of site preparation on emergence and early establishment of *Larix olgensis*, in montane regions of northeastern China. *New For.* **2008**, *36*, 247–260. [[CrossRef](#)]
58. Wei, H.X.; Xu, C.Y.; Hawkins, B.J.; Ma, L.; Jiang, L. Organic amendment and inorganic fertilization affect soil properties and quality of *Larix olgensis* bareroot stock. *New For.* **2012**, *43*, 155–168. [[CrossRef](#)]
59. Zhu, Y.; Dumroese, R.K.; Pinto, J.R.; Li, G.L.; Liu, Y. Fall fertilization enhanced nitrogen storage and translocation in *Larix olgensis*, seedlings. *New For.* **2013**, *44*, 849–861. [[CrossRef](#)]
60. Eguchi, N.; Fukatsu, E.; Funada, R.; Tobita, H.; Kitao, M.; Maruyama, Y.; Koike, T. Changes in morphology, anatomy, and photosynthetic capacity of needles of Japanese Larch (*Larix kaempferi*) seedlings grown in high CO₂ concentrations. *Photosynthetica* **2004**, *42*, 173–178. [[CrossRef](#)]
61. Mao, Q.Z.; Watanabe, M.; Imori, M.; Kim, Y.S.; Kita, K.; Koike, T. Photosynthesis and nitrogen allocation in needles in the sun and shade crowns of hybrid larch saplings: Effect of nitrogen application. *Photosynthetica* **2012**, *50*, 422–428. [[CrossRef](#)]
62. Wang, W.J.; Watanabe, Y.; Endo, I.; Kitaoka, S.; Koike, T. Seasonal changes in the photosynthetic capacity of cones on a larch (*Larix kaempferi*) canopy. *Photosynthetica* **2006**, *44*, 345–348. [[CrossRef](#)]
63. Galvagno, M.; Rossini, M.; Migliavacca, M.; Cremonese, E.; Colombo, R.; Morra-di-Cella, U. Seasonal course of photosynthetic efficiency in *Larix decidua* Mill. in response to temperature and change in pigment composition during senescence. *Int. J. Biometeorol.* **2013**, *57*, 871–880. [[CrossRef](#)] [[PubMed](#)]

64. Kurachi, N.; Hagihara, A.; Hozumi, K. Canopy photosynthetic production in a Japanese larch stand. I. Seasonal and vertical changes of leaf characteristics along the light gradient in a canopy. *Ecol. Res.* **1992**, *7*, 255–265. [[CrossRef](#)]
65. Liu, Q.; Dong, L.H.; Li, F.R.; Li, X. Spatial heterogeneity of canopy photosynthesis for *Larix olgensis*. *Chin. J. Appl. Ecol.* **2016**, *27*, 2789–2796. (In Chinese)
66. Wu, C.; Wang, Z.X.; Sun, H.L.; Guo, S.L. Effects of different concentrations of Nitrogen and Phosphorus on Chlorophyll Biosynthesis, Chlorophyll a Fluorescence, and Photosynthetic Rate in *Larix olgensis* seedlings. *Sci. Silv. Sin.* **2005**, *41*, 31–36. (In Chinese)
67. Zhao, X.Z.; Jiang, H.F.; Mao, Z.J. The studies of the photosynthetic characteristics of *Larix olgensis* Herry., *Larix kaempferi* Carr. and *Larix gmelinii* Rupr. seedlings. *Bull. Bot. Res.* **2007**, *27*, 361–366. (In Chinese)
68. Luca, T.H.D. Relationship of 0.5 M K₂SO₄ extractable anthrone-reactive carbon to indices of microbial activity in forest soils. *Soil Biol. Biochem.* **1998**, *30*, 1293–1299. [[CrossRef](#)]
69. Cluzeau, C.; Goff, N.L.; Ottorini, J.M. Development of primary branches and crown profile of *Fraxinus excelsior*. *Can. J. For. Res.* **1994**, *24*, 2315–2323. [[CrossRef](#)]
70. Bassman, J.H.; Zwier, J.C. Gas exchange characteristics of *Populus trichocarpa*, *Populus deltoides* and *Populus trichocarpa* × *P. deltoides* clones. *Tree Physiol.* **1991**, *8*, 145–159. [[CrossRef](#)] [[PubMed](#)]
71. Lloyd, J.; Taylor, J.A. On the Temperature dependence of soil respiration. *Funct. Ecol.* **1994**, *8*, 315–323. [[CrossRef](#)]
72. Rodríguez-calcerrada, J.; Atkin, O.K.; Robson, T.M.; Zaragoza-castells, J.; Gil, L.; Aranda, I. Thermal acclimation of leaf dark respiration of beech seedlings experiencing summer drought in high and low light environments. *Tree Physiol.* **2010**, *30*, 214–224. [[CrossRef](#)] [[PubMed](#)]
73. Weerasinghe, L.K.; Creek, D.; Crous, K.Y.; Xiang, S.; Liddell, M.J.; Turnbull, M.H.; Atkin, O.K. Canopy position affects the relationships between leaf respiration and associated traits in a tropical rainforest in Far North Queensland. *Tree Physiol.* **2014**, *34*, 564–584. [[CrossRef](#)] [[PubMed](#)]
74. Meyer, N.; Meyer, H.; Welp, G.; Amelung, W. Soil respiration and its temperature sensitivity (Q₁₀): Rapid acquisition using mid-infrared spectroscopy. *Geoderma* **2018**, *323*, 31–40. [[CrossRef](#)]
75. Sage, R.F.; Kubien, D.S. The temperature response of C₃ and C₄ photosynthesis. *Plant Cell Environ.* **2007**, *30*, 1086–1106. [[CrossRef](#)] [[PubMed](#)]
76. Way, D.A.; Sage, R.F. Thermal acclimation of photosynthesis in black spruce [*Picea mariana* (Mill.) B.S.P.]. *Plant Cell Environ.* **2008**, *31*, 1250–1262. [[CrossRef](#)] [[PubMed](#)]
77. Wieser, G.; Oberhuber, W.; Walder, L.; Spieler, D.; Gruber, A. Photosynthetic temperature adaptation of *Pinus cembra*, within the timberline ecotone of the Central Austrian Alps. *Ann. For. Sci.* **2010**, *67*, 201. [[CrossRef](#)] [[PubMed](#)]
78. Calama, R.; Puértolas, J.; Madrigal, G.; Pardos, M. Modeling the environmental response of leaf net photosynthesis in *Pinus pinea* L. natural regeneration. *Ecol. Model.* **2013**, *251*, 9–21. [[CrossRef](#)]
79. Mayoral, C.; Calama, R.; Sánchez-González, M.; Pardos, M. Modelling the influence of light, water and temperature on photosynthesis in young trees of mixed Mediterranean forests. *New For.* **2015**, *46*, 485–506. [[CrossRef](#)]
80. Lloyd, J.; Farquhar, G.D. Effects of rising temperatures and [CO₂] on the physiology of tropical forest trees. *Phil. Trans. Biol. Sci.* **2008**, *363*, 1811–1817. [[CrossRef](#)] [[PubMed](#)]
81. Hikosaka, K.; Nabeshima, E.; Hiura, T. Seasonal changes in the temperature response of photosynthesis in canopy leaves of *Quercus crispula* in a cool-temperate forest. *Tree Physiol.* **2007**, *27*, 1035–1041. [[CrossRef](#)] [[PubMed](#)]
82. Tjoelker, M.G.; Oleksyn, J.; Reich, P.B. Modelling respiration of vegetation: Evidence for a general temperature-dependent Q₁₀. *Glob. Chang. Biol.* **2001**, *7*, 223–230. [[CrossRef](#)]
83. Griffin, K.L.; Tissue, D.T.; Turnbull, M.H.; Schuster, W.; Whitehead, D. Leaf dark respiration as a function of canopy position in *Nothofagus fusca* trees grown at ambient and elevated CO₂ partial pressures for 5 years. *Funct. Ecol.* **2001**, *15*, 497–505. [[CrossRef](#)]
84. Griffin, K.L.; Turnbull, M.; Murthy, R. Canopy position affects the temperature response of leaf respiration in *Populus deltoides*. *New Phytol.* **2002**, *154*, 609–619. [[CrossRef](#)]
85. Tissue, D.T.; Lewis, J.D.; Wullschlegel, S.D.; Amthor, J.S.; Griffin, K.L.; Anderson, O.R. Leaf respiration in sweetgum (*Liquidambar styraciflua*) at different canopy positions grown in ambient and elevated CO₂ in the field. *Tree Physiol.* **2002**, *22*, 1157–1166. [[CrossRef](#)] [[PubMed](#)]

86. Lewis, J.D.; Lucash, M.; Olszyk, D.; Tingey, D.T. Seasonal patterns of photosynthesis in Douglas-fir seedlings during the third and fourth year of exposure to elevated CO₂, and temperature. *Plant Cell Environ.* **2001**, *24*, 539–548. [[CrossRef](#)]
87. Sperlich, D.; Chang, C.T.; Penuelas, J.; Gracia, C.; Sabaté, S. Seasonal variability of foliar photosynthetic and morphological traits and drought impacts in a Mediterranean mixed forest. *Tree Physiol.* **2015**, *35*, 501–520. [[CrossRef](#)] [[PubMed](#)]
88. Mitamura, M.; Yamamura, Y.; Nakano, T. Large-scale canopy opening causes decreased photosynthesis in the saplings of shade-tolerant conifer, *Abies veitchii*. *Tree Physiol.* **2009**, *29*, 137–145. [[CrossRef](#)] [[PubMed](#)]
89. Richardson, A.D.; Berlyn, G.P.; Ashton, P.M.S.; Thadani, R.; Cameron, I.R. Foliar plasticity of hybrid spruce in relation to crown position and stand age. *Can. J. Bot.* **2000**, *78*, 305–317.
90. Zhang, Y.; Zheng, Q.; Tyree, M.T. Factors controlling plasticity of leaf morphology in *Robinia pseudoacacia* L. I: Height-associated variation in leaf structure. *Ann. For. Sci.* **2012**, *69*, 29–37. [[CrossRef](#)]
91. Zhang, Y.X.; Equiza, M.A.; Zheng, Q.S.; Tyree, M.T. Factors controlling plasticity of leaf morphology in *Robinia pseudoacacia* L. II: The impact of water stress on leaf morphology of seedlings grown in a controlled environment chamber. *Ann. For. Sci.* **2012**, *69*, 39–47. [[CrossRef](#)]
92. Xu, C.Y.; Griffin, K.L. Seasonal variation in the temperature response of leaf respiration in *Quercus rubra*: Foliage respiration and leaf properties. *Funct. Ecol.* **2006**, *20*, 778–789. [[CrossRef](#)]
93. Yuko, Y.; Kouki, H.; Tadaki, H. Seasonal changes in photosynthesis, nitrogen content and nitrogen partitioning in *Lindera umbellata* leaves grown in high or low irradiance. *Tree Physiol.* **2006**, *26*, 1315–1323.
94. Radoglou, K.; Teskey, R.O. Changes in rates of photosynthesis and respiration during needle development of loblolly pine. *Tree Physiol.* **1997**, *17*, 485–488. [[CrossRef](#)] [[PubMed](#)]
95. Collier, D.E.; Thibodeau, B.A. Changes in respiration and chemical content during autumnal senescence of *Populus tremuloides* and *Quercus rubra* leaves. *Tree Physiol.* **1995**, *15*, 759–764. [[CrossRef](#)] [[PubMed](#)]
96. Vose, J.M.; Ryan, M.G. Seasonal respiration of foliage, fine roots, and woody tissues in relation to growth, tissue N, and photosynthesis. *Glob. Chang. Biol.* **2010**, *8*, 182–193. [[CrossRef](#)]



© 2018 by the authors. Licensee MDPI, Basel, Switzerland. This article is an open access article distributed under the terms and conditions of the Creative Commons Attribution (CC BY) license (<http://creativecommons.org/licenses/by/4.0/>).